

Carrier recombination in sonochemically synthesized ZnO powders

M.I. ZAKIROV*, O.A. KOROTCHENKOV

Taras Shevchenko Kiev National University, 64/13 Vladimirskaya St., Kiev, 01601, Ukraine

ZnO powders with particle size in the nm to μm range have been fabricated by sonochemical method, utilizing zinc acetate and sodium hydroxide as starting materials. Carrier recombination processes in the powders have been investigated using the photoluminescence, FT-IR and surface photovoltage techniques. It has been shown that the photoluminescence spectra exhibit a number of defect-related emission bands which are typically observed in ZnO lattice and which depend on the sonication time. It has been found that the increase of the stirring time results in a faster decay of the photovoltage transients for times shorter than approximately 5 ms. From the obtained data it has been concluded that the sonication modifies the complicated trapping dynamics from volume to surface defects, whereas the fabrication method itself offers a remarkably convenient means of modifying the relative content of the surface-to-volume defect ratio in powder grains and altering the dynamics of photoexcited carriers.

Keywords: ZnO; sonochemical synthesis; surface photovoltage; photoluminescence

© Wrocław University of Science and Technology.

1. Introduction

ZnO is a wide band gap semiconductor with a high exciton binding energy which attracts considerable scientific and applied interest with respect to exploiting its optical properties [1–5]. For example, high thermal and chemical stability, simple tunability of the optical and electrical properties are widely applicable in optoelectronic devices [6, 7]. Moreover, while exhibiting an excitonic emission peak in the ultraviolet (UV) region, ZnO typically shows strong visible luminescence bands which are due to numerous point defects present in the lattice [8–11]. Due to these facts, various methods of producing zinc oxide with different morphology and point defect content have been developed so far [12].

Quite recently, the synthesis of nanoscale materials under microwave irradiation and during sonochemical reactions became particularly attractive [13–17]. The main effect of sonochemical reaction is cavitation which is accompanied by the formation, growth and collapse

of cavitation bubbles. Inside the collapsing bubble, extreme physical and chemical conditions (temperatures ≥ 5000 K and pressures ≥ 1800 MPa) are realized [18–20]. With the chemical synthesis, metal oxides are generally grown from their acetate precursors [21–23]. Employing sonochemical reactions, a low-vapor-pressure metal acetate is usually dissolved in solvents to form a homogenous solution. Consequently, numerous metal oxide materials were successfully synthesized in sonochemical reactions and, particularly, ZnO, CuO, Co_3O_4 and Fe_3O_4 nanocrystals were sonochemically produced from respective acetate compounds in various solutions [23].

In this work, a simple sonochemical route of producing ZnO powder materials is presented and it is also shown that in those materials, concentration of defects can be changed by varying the reaction conditions.

2. Experimental

For sonochemical synthesis of ZnO, zinc acetate and sodium hydroxide were used as starting

*E-mail: zakyrov@gmail.com

materials. 2-propanol was used to dissolve these materials and obtain a liquid solution. At first, 0.10 g of zinc acetate was dissolved in 25 mL of 2-propanol and the resulting solution was added to 125 mL of cooled 2-propanol. Next, 15 mL of 0.050 M sodium hydroxide in isopropanol was prepared. Finally, the sodium hydroxide solution was slowly added into 2-propanol and zinc acetate solution. The final solution was transferred into the ultrasound reactor, allowing it to achieve cavitation conditions. Details of the ultrasonic setup are given in the literature [24]. When the synthesis was finished, the resulting product was continuously washed in methanol and water and dried in ambient air. The white powder, obtained in this process, was then dissolved in 2-propanol (IPA). The grain size in the powder was found to vary in the range of a few dozens of nm to $\sim 130 \mu\text{m}$. In this work, the samples of ZnO powders are marked as SC1, SC2 and SC3 respectively. Subsequently, these samples are compared according to their stirring time of 1 min, 60 min and 120 min, respectively.

Photoluminescence (PL) spectra and decays were recorded at room temperature using a monochromator MDR-4 and a photomultiplier tube FEU-79 with a computer data acquisition system. PL decays were analyzed with use of a digital oscilloscope GDS-806S with a time resolution of $1 \mu\text{s}$. An N_2 laser with the wavelength of $\lambda = 337.2 \text{ nm}$ (3.67 eV) was used as the photogeneration source [25]. Surface photovoltage (SPV) decays were measured in the contactless capacitor arrangement, and details of the setup are given in the literature [26]. Fourier transform infrared (FT-IR) spectra were recorded using FT-IR Spectrometer SPECTRUM BX II (Perkin Elmer).

3. Results and discussion

3.1. PL spectra

Photoluminescence spectra of SC1, SC2 and SC3 samples are shown in Fig. 1. They can be decomposed into two components (dashed lines) with relative intensities given by the vertical bars. It is seen that a strong yellow PL band peaked in the wavelength range from about 590 nm to 650 nm

is observed in all the samples. It is also seen that prolonged sonication times make the PL spectral shape narrower, as evidenced by comparing the spectrum in Fig. 1c with the spectra in Fig. 1a and Fig. 1b, and the shift of the second emission band to the green spectral range which arises at 567 nm in Fig. 1c.

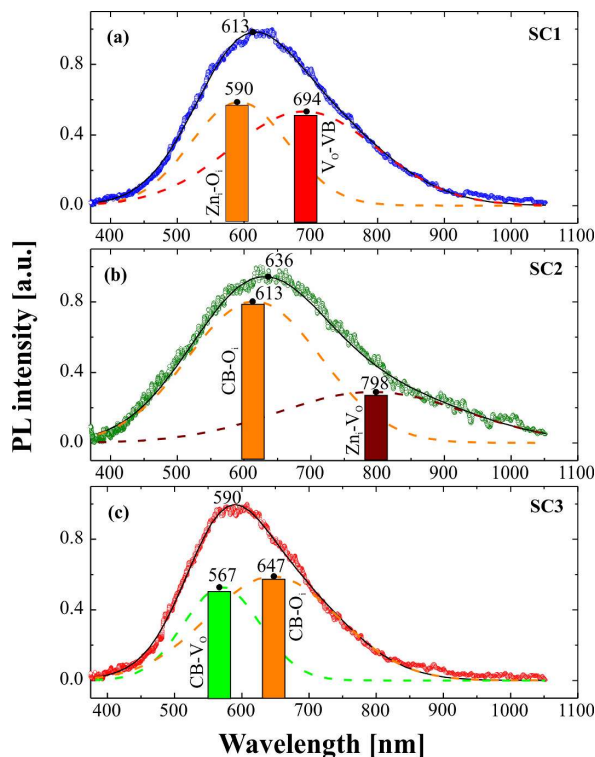


Fig. 1. PL spectra (points) and decomposed spectral bands (dashed) in sonochemically synthesized SC1, SC2 and SC3 samples. Solid line presents the sum of the two dashed spectral shapes.

It is quite obvious that the observed changes are due to complicated defect chemistry relevant to the sonochemical processing. As reported in the literature [1, 10, 27–29], room-temperature PL of ZnO can exhibit one emission peak in the UV region which is due to the recombination of free excitons, and one or more peaks in the visible region. The latter ones are commonly associated with the defect-related emissions, such that the defect properties strongly affect optical spectra of ZnO. Intrinsic and extrinsic point defects are generally distinguished with respect to their localization in the bulk and at the surface of ZnO, respectively.

We, therefore, summarize the band decomposition parameters and the electronic transitions which are responsible for the observed bands in Table 1. Here, we use the notation for identifying the starting and the final states which are as follows: Zn_i – interstitial zinc, O_i – interstitial oxygen, V_o – oxygen vacancy, CB and VB – conduction and valence band, respectively.

Weighing the observed spectral changes it can be concluded that the sonication modifies the relative content of the surface-to-volume defect ratio. Of further significance is the fact that the observed growth of the green band with increasing sonication time is fully consistent with the reported values of the defect formation energies E which are related to each other as follows: $E(V_{Zn}) < E(V_O) < E(Zn_i) < E(ZnO) < E(O_i) < E(O_{Zn})$ [40].

3.2. FT-IR spectra

In order to detect the surface species and the nature of surface chemical bonds, consider FT-IR spectra of the samples which are shown in Fig. 2. They exhibit a number of strong absorption peaks relevant to IPA (dotted spectrum). A number of subsidiary bands appears in the SC1, SC2 and SC3 samples in the spectral regions marked by ellipse 1 to ellipse 3 in Fig. 2. In general, electrostatic passivation of surface cations by negatively charged ligands occurs in II-VI semiconductor nanoparticles [41] which is capable of explaining consistently the observed changes in the FT-IR spectra of ZnO particles.

As can be seen in Fig. 2, the characteristic absorption band at about 510 cm^{-1} is detected in all samples and it is attributed to the Zn–O bonds [42]. Furthermore, the transmission gradually decreases in the region from 3000 cm^{-1} to 3500 cm^{-1} (region 3 in Fig. 2) which indicates the more pronounced role of the $\nu(\text{O–H})$ vibration mode in the spectra of the samples produced with longer stirring time. Indeed, the broad absorption peak centered at 3342 cm^{-1} corresponds to the –OH group of IPA. For our SC samples, this band shifts to 3350 cm^{-1} . Moreover, a small shoulder at $\sim 1650\text{ cm}^{-1}$ (region 2) is resolved in all SC samples, and it is assigned to the O–H stretching

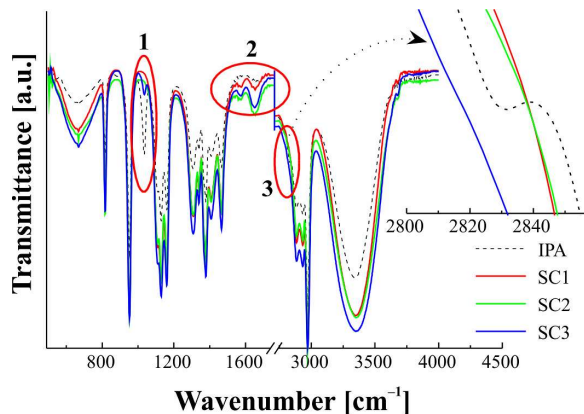


Fig. 2. FT-IR transmission spectra of sonochemically fabricated ZnO powders dissolved in IPA.

vibrations of water molecules or moisture adsorbed on the ZnO surface [42]. Additionally, the FT-IR spectrum in the C–H vibration range (region 3 in Fig. 2) is enlarged in the inset of Fig. 2. One can see that the peak at 2830 cm^{-1} observed in IPA completely vanishes in our SC synthesized samples of ZnO powders. The peak at 1600 cm^{-1} is usually attributed to either O–H stretching vibrations of hydroxyl functional groups or to the bending vibrations of the surface H–OH, which shows that hydroxyl groups are adsorbed on the surface of ZnO [43]. Finally, the most pronounced changes in FT-IR spectra are monitored in region 1 of Fig. 2. The peak at 1035 cm^{-1} in alcohols is related to the C–O stretching vibrations. This peak is clearly detectable in pure IPA but quenches remarkably in the SC samples.

The spectral changes observed in Fig. 2 can be explained by assuming that a molecule of IPA is absorbed on the surface of ZnO and then interacts with the surface of the grain via O atoms. It is interesting that the similar conclusion can be drawn from the data describing the synthesis of gold and silver nanoparticles passivated by PVP [44–47].

Therefore, the data in Fig. 2 show that the main changes in FT-IR spectra of IPA are associated with the change in transmittance of the (O–X) bond in IPA molecules. Passivation of ZnO particles in IPA is realized by the interaction of the oxygen atom in IPA and zinc in ZnO. Taking

Table 1. Decomposed band parameters and peak attribution for the PL spectra given in Fig. 1.

Sample	Peak position of the decomposed band [nm]	Type of transition responsible for the band	Intensity of the decomposed band normalized to the maximum peak value	Literature
SC1	589	$Zn_i \rightarrow O_i$ (CB- O_i)	0.58	[30–33]
	693	$V_o \rightarrow VB$	0.53	[31, 34]
SC2	612	$CB \rightarrow O_i$ (Zn_i - O_i)	0.80	[31, 33, 35]
	797	$Zn_i \rightarrow V_o$ (CB- V_o)	0.28	[30, 34]
SC3	566	$CB \rightarrow V_o$ (Zn_i - V_o)	0.52	[36–39]
	647	$CB \rightarrow O_i$	0.59	[10, 31]

this scenario into account, it can be expected that the concentration of oxygen vacancies in SC samples will vary with varying stirring time which, in turn, can be taken into account, when analyzing the PL spectral changes given in Fig. 1.

3.3. SPV and PL decays

Based on the above analysis and previously demonstrated strong correlation between the surface defects and optoelectronic properties of ZnO materials [28, 48–50], one can expect that the SPV decays would be remarkably different in the SC samples obtained at different stirring times. This is exactly what is seen in Fig. 3. In this figure, normalized SPV decays in SC1, SC2 and SC3 samples are shown. The main observation is that the increase in the stirring time (from sample SC1 to SC3) is accompanied by accelerated initial time decays in the SPV transients shortly after excitation (for times shorter than ≈ 5 ms in curve 1 to curve 3, respectively). These are followed by a longer nearly exponential decay component for times longer than 5 ms. This component remains practically unchanged with increasing the stirring time.

It is well known that SPV decays depend on several factors, such as (i) lifetime of photogenerated charges with respect to their recombination pathways which, in turn, determines the PL intensity, (ii) concentration of surface defects, (iii) efficiency of the inter-particle charge transfer. It seems to be very likely that the data shown in Fig. 3 indicate that the free carriers trapping dynamics is

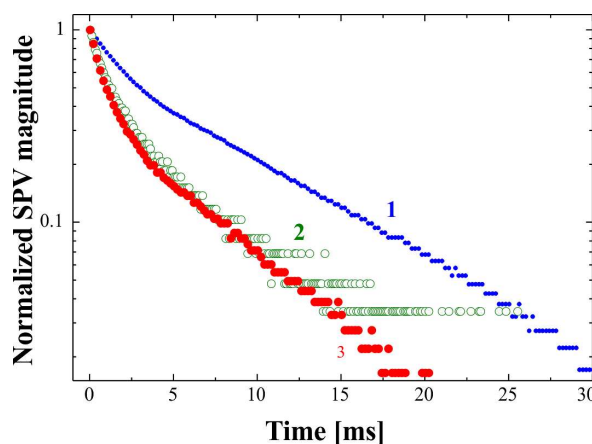


Fig. 3. SPV decays of sonochemically synthesized SC1 (1), SC2 (2) and SC3 (3) samples.

mainly determined by decreasing of the surface defect concentration, provided that the distribution of the grain sizes shifts to smaller values in the sequence of SC1, SC2 and SC3 samples, respectively. This conclusion is supported by the results presented in Section 3.2., where we showed that the concentration of surface defects decreases with increasing stirring time. It is, therefore, believed that ZnO particles fabricated at short stirring times have rather high concentration of surface defects. These defects act as traps for photogenerated charges, slowing down the SPV decay. Prolonged stirring times improve the quality of the particle surface, so that the trap concentration decreases which leads to marked acceleration of the initial SPV decay.

The latter conclusion is also supported by analyzing the PL decays shown in Fig. 4. Indeed, no

difference is found in the decay curve shapes reproduced in samples SC1 and SC3 which implies that the surface states do not seem to be involved into the PL emission process.

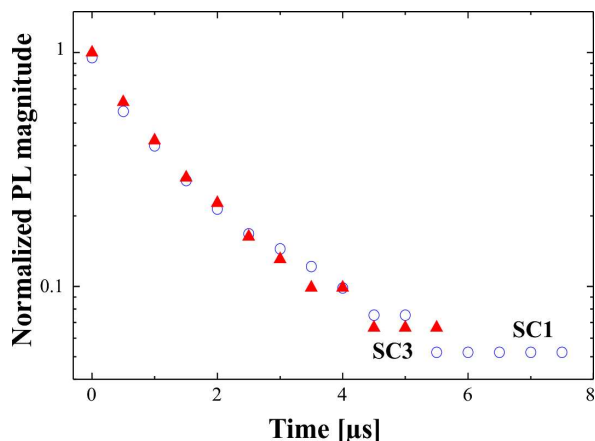


Fig. 4. Time resolved PL decays of SC1 (circles) and SC3 (triangles) samples.

4. Conclusions

In conclusion, the carrier recombination processes in sonochemically synthesized ZnO powder particles have been investigated using PL, FT-IR and SPV techniques. It has been shown that the PL spectra were rather sensitive function of the stirring time during the ultrasonic bath. A number of defect-related PL bands, typical of ZnO lattice, has been detected, and each of the PL band was decomposed into a sum of two partially overlapping subbands. The performed measurements indicate that the sonochemical fabrication route of producing ZnO gives convenient means of the modification of the ratio surface-to-volume defect concentrations.

References

- [1] DJURIŠIĆ A.B., LEUNG Y.H., TAM K.H., HSU Y.F., DING L., GE K., ZHONG Y.C., WONG K.S., CHAN W.K., TAM H.L., CHEAH K.W., KWOK W.M., PHILLIPS D.L., *Nanotechnology*, 18 (2007), 095702.
- [2] KWOK W.M., DJURIŠIĆ A.B., LEUNG Y.H., CHAN W.K., PHILLIPS D.L., *Appl. Phys. Lett.*, 878 (2005), 09310.
- [3] STUDENIKIN S.A., COCIVERA M., *J. Appl. Phys.*, 91 (2002), 5060.
- [4] PRILLER H., DECKER M., HAUSCHILD R., KALT H., KLINGSHIRN C., *Appl. Phys. A-Mater.*, 86 (2005), 111909.
- [5] JANA A., SUJATHA DEVI., MITRA A., BANDYOPADHYAY N.R., *Mater. Chem. Phys.*, 139 (2013), 431.
- [6] DJURIŠIĆ A.B., CHEN X., LEUNG Y.H., MAN CHING NG A., *J. Mater. Chem.*, 22 (2012), 6526.
- [7] ABDULGAFOUR H.I., HASSAN Z., AHMED N.M., YAM F.K., *J. Appl. Phys.*, 112 (2012), 074510.
- [8] ZHAO L.-H., ZHANG J., SUN S.-Q., *J. Lumin.*, 132 (2012), 2595.
- [9] PENG Y., WANG Y., CHEN Q.-C., ZHU Q., XU A.W., *CrystEngComm*, 16 (2014), 7906.
- [10] DJURIŠIĆ A.B., LEUNG Y.H., TAM K.H., *Appl. Phys. Lett.*, 88 (2006), 103107.
- [11] JANOTTI A., VAN DE WALLE C.G., *Phys. Rev. B*, 76 (2007), 165202.
- [12] SONG R., LIU Y., HE L., *Solid State Sci.*, 10 (2008), 1563.
- [13] BHATTE K.D., FUJITA S.I., ARAI M., PANDIT A.B., BHANAGE B.M., *Ultrason. Sonochem.*, 18 (2011), 54.
- [14] HOSNI M., FARHAT S., SCHOENSTEIN F., KARMOUS F., JOUINI N., VIANA B., MGAIDI A., *J. Alloy. Compd.*, 615 (2013), 10.
- [15] BANERJEE P., CHAKRABARTI S., MAITRA S., DUTTA B.K., *Ultrason. Sonochem.*, 19 (2012), 85.
- [16] CHATEL G., MACFARLANE D.R., *Chem. Soc. Rev.*, 43 (2014), 8132.
- [17] PANG Y.L., ABDULLAH A.Z., BHATIA S., *Desalination*, 277 (2011), 1.
- [18] BANG J.H., SUSLICK K.S., *Adv. Mater.*, 22 (2010), 1039.
- [19] KHORSAND Z.A., MAJID W.H.A., WANG H.Z., YOUSEFI R., MORADI G.A., REN Z.F., *Ultrason. Sonochem.*, 20 (2013), 395.
- [20] PANDA N.R., SAHU D., ACHARYA B.S., NAYAK P., *Curr. Appl. Phys.*, 15 (2015), 389.
- [21] LAURENT S., FORGE D., PORT M., ROCH A., ROBIC C., ELST L.V., MULLER R.N., *Chem. Rev.*, 108 (2008), 2064.
- [22] VIJAYA KUMAR R., ELGAMIEL R., DIAMANT Y., GEDANKEN A., NORWIG J., *Langmuir*, 17 (2001), 1406.
- [23] KUMAR V.R., DIAMANT Y., GEDANKEN A., *Chem. Mater.*, 12 (2000), 2301.
- [24] PODOLIAN A., NADTOCHIY A., KURYLIUK V., KOROTCHENKOV O., SCHMID J., DRAPALIK M., SCHLOSSER V., *Sol. Energ. Mat. Sol. C.*, 95 (2011), 765.
- [25] VERETEL'NIK M.B., KOROTCHENKOV O.A., KURYLIUK V.V., NADTOCHII A.B., *Tech. Phys. Lett.*, 39 (2013), 744.
- [26] PODOLIAN A., KOZACHENKO V., NADTOCHIY A., BOROVOY N., KOROTCHENKOV O., *J. Appl. Phys.*, 107 (2010), 093706.
- [27] GOMI M., OOHIRA N., OZAKI K., KOYANO M., *Jpn. J. Appl. Phys.*, 42 (2003), 481.
- [28] SHALISH I., TEMKIN H., NARAYANAMURTI V., *Phys. Rev. B*, 69 (2004), 245401.

- [29] ZHOU H., ALVES H., HOFMANN D.M., KRIEGSEIS W., MEYER B.K., KACZMARCZYK G., HOFFMANN A., *Appl. Phys. Lett.*, 80 (2002), 210.
- [30] LIN B., FU Z., JIA Y., *Appl. Phys. Lett.*, 79 (2001), 943.
- [31] ALVI N.H., UL HASAN K., NUR O., WILLANDER M., *Nanoscale Res. Lett.*, 6 (2011), 130.
- [32] ZHENG J., CAO S., WANG L., GAO F., *RSC Adv.*, 4 (2014), 30948.
- [33] CAO B., CAI W., ZENG H., *Appl. Phys. Lett.*, 88 (2006), 161101.
- [34] JANOTTI A., WALLE VAN DE C.G., *Phys. Rev. B*, 76 (2007), 127.
- [35] MAROTTI R.E., BADÁN J.A., QUAGLIATA E., DALCHIELE E.A., *Physica B*, 398 (2007), 337.
- [36] TAY Y.Y., TAN T.T., BOEY F., LIANG M., YE J., ZHAO Y., NORBY T., LI S., *Phys. Chem. Chem. Phys.*, 12 (2010), 2373.
- [37] DJURISÍĆ A.B., LEUNG Y.H., TAM K.H., DING L., GE W.K., CHEN Y.H., GWO S., *Appl. Phys. Lett.*, 88 (2006), 103107.
- [38] AHN C.H., KIM Y.Y., KIM D.C., MOHANTA S.K., CHO H.K., *J. Appl. Phys.*, 105 (2009), 013502.
- [39] YE J.D., GU S.L., QIN F., ZHU S.M., LIU S.M., ZHOU X., LIU W., HU L.Q., ZHANG R., SHI Y., ZHENG Y.D., *Appl. Phys. A-Mater.*, 81 (2005), 759.
- [40] JANOTTI A., WALLE VAN DE C.G., *Rep. Prog. Phys.*, 72 (2009), 126501.
- [41] GILBERT B., HUANG F., LIN Z., GOODELL C., ZHANG., BANFIELD J.F., *Nano Lett.*, 6 (2006), 605.
- [42] AMEEN S., AKHTAR M.S., SHIN H.S., *Chem. Eng. J.*, 195 (2012), 307.
- [43] MOUSSAWI R.N., PATRA D., *RSC Adv.*, 6 (2016), 17256.
- [44] BEHERA M., RAM S., *Int. Nano Lett.*, 3 (2013), 17.
- [45] HOPPE C.E., LAZZARI M., PARDIÑAS-BLANCO I., LÓPEZ-QUINTELA M.A., *Langmuir*, 22 (2006), 7027.
- [46] BEHERA M., RAM S., *Appl. Nanosci.*, 3 (2012), 83.
- [47] BORODKO Y., HABAS S.E., KOEBEL M., YANG P., FREI H., SOMORJAI G.A., *J. Phys. Chem. B*, 110 (2006), 23052.
- [48] PHOLNAK C., SIRISATHITKUL C., SUWANBOON S., HARDING D.J., *Mat. Res.*, 17 (2014), 405.
- [49] LIQIANG J., XIAOJUN S., JING S., WEIMIN C., ZILI X., YAOGUO D., HONGGANG F., *Sol. Energ. Mat. Sol. C.*, 79 (2003), 133.
- [50] WANG Z.G., ZU X.T., ZHU S., WANG L.M., *Physica E*, 35 (2006), 199.

Received 2016-03-22

Accepted 2016-12-18